

ОБЪЕДИНЕННЫЙ  
ИНСТИТУТ  
ЯДЕРНЫХ  
ИССЛЕДОВАНИЙ  
ДУБНА

E7-94-80

Yu.A.Lazarev, Yu.V.Lobanov, Yu.Ts.Oganessian,  
V.K.Utyonkov, F.Sh.Abdullin, G.V.Buklanov, B.N.Gikal,  
S.Iliev, A.N.Mezentsev, A.N.Polyakov, I.M.Sedykh,  
I.V.Shirokovsky, V.G.Subbotin, A.M.Sukhov,  
Yu.S.Tsyganov, V.E.Zhuchko, R.W.Lougheed\*,  
K.J.Moody\*, J.F.Wild\*, E.K.Hulet\*, J.H.McQuaid\*

DISCOVERY OF ENHANCED NUCLEAR  
STABILITY NEAR THE DEFORMED SHELLS  
 $N=162$  AND  $Z=108$

Submitted to «Physical Review Letters»

---

\*University of California, Lawrence Livermore National  
Laboratory, Livermore, CA 94551, USA

1994

Обнаружение повышенной стабильности ядер  
вблизи деформированных оболочек  $N = 162$  и  $Z = 108$

В реакции  $^{248}\text{Cm} + ^{22}\text{Ne}$  синтезированы два новых изотопа,  $^{265}106$  и  $^{266}106$ . Они идентифицированы методом наблюдения генетической связи между их  $\alpha$ -распадом и  $\alpha$ -распадом или спонтанным делением дочерних ядер. Измерены значение  $E_\alpha = 8,63 \pm 0,05$  МэВ для  $^{266}106$  и период полураспада  $1,2^{+1,0}_{-0,5}$  с для дочернего ядра  $^{262}104$ . Для  $^{265}106$  измерено  $E_\alpha = 8,71 - 8,91$  МэВ. Оценки времен жизни относительно  $\alpha$ -распада составляют 10-30 с для  $^{266}106$  и 2-30 с для  $^{265}106$ , а ветви на спонтанное деление не превышают 50%. Наблюдаемые радиоактивные свойства  $^{266}106$  обнаруживают повышенную стабильность ядер вблизи теоретически предсказанных деформированных оболочек  $N = 162$  и  $Z = 108$ .

Работа выполнена в Лаборатории ядерных реакций ОИЯИ.

Препринт Объединенного института ядерных исследований. Дубна, 1994

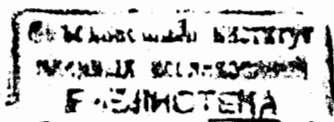
Discovery of Enhanced Nuclear Stability near the Deformed  
Shells  $N = 162$  and  $Z = 108$

In bombardments of  $^{248}\text{Cm}$  with  $^{22}\text{Ne}$  we discovered two new isotopes,  $^{265}106$  and  $^{266}106$ , by establishing genetic links between their  $\alpha$  decays and SF or  $\alpha$  decays of the daughter nuclides. We measured  $E_\alpha = 8.63 \pm 0.05$  MeV for  $^{266}106$  and a half-life of  $1.2^{+1.0}_{-0.5}$  s for its daughter  $^{262}104$ . For  $^{265}106$  we measured  $E_\alpha = 8.71$  to  $8.91$  MeV. We estimated  $\alpha$  half-lives of 10-30 s for  $^{266}106$  and 2-30 s for  $^{265}106$ , and SF branches of 50% or less. The decay properties of  $^{266}106$  establish the existence of enhanced nuclear stability near the predicted deformed shells  $N = 162$  and  $Z = 108$ .

The investigation has been performed at the Laboratory of Nuclear Reactions, JINR.

Recent macroscopic-microscopic calculations (see, e.g., Refs. [1,2,3,4,5]) all show a large negative shell correction for the ground states of nuclei at and near  $N=162$  and  $Z=108$  due to a large gap in the Nilsson levels between  $N=162$  and  $163$  and  $Z=108$  and  $109$ , which is further enhanced by considering higher order multipolarities of deformed shapes, particularly the hexadecapole vibration. However, spontaneous fission (SF) is usually the limiting decay mode for even-even nuclides in this region and estimations of SF half-lives from barrier penetration probabilities vary by many orders of magnitude. Although the calculated static barrier heights are about equal, differences in half-life estimates can be attributed to differing assumptions regarding the dynamical path through the fission barrier and the consequent inertial mass. For example, Möller *et al.* [5], taking  $^{258}\text{Fm}$  as a model for heavier nuclei, assume that the path after the first barrier is short with the emerging fragments being nearly spherical and close to the doubly magic  $^{132}\text{Sn}$ . On the other hand, Patyk, Sobiczewski, *et al.* [2-4] calculate dynamical barriers that show a different path, higher inertial mass, and consequently much longer SF half-lives. This competition between static and dynamic features of the SF process which lead to such large differences in stability makes experiments that explore ground-state decay properties of nuclei around  $N=162$  and  $Z=108$  one of the most important tasks in heavy element research.

We report here on our experiments resulting in the first direct evidence of nuclear stability near the predicted deformed shells by producing the even-even  $N=160$  nuclide  $^{266}106$  (and also  $^{265}106$ ). The only previously known nu-



clide with  $N=160$ , the 5-ms isotope  $^{262}106$ , provided a hint of unexpected stability against SF [6]. Prior to our work, four isotopes of element 106 had been identified. These are the odd- $A$   $\alpha$ -emitters  $^{259}106$  [7],  $^{261}106$  [7], and  $^{263}106$  [8], with half-lives in the range of 0.3 to 0.9 s, and the 3.6-ms even-even  $^{260}106$  [7,9,10] which has a SF branch of  $50^{+30}_{-20}\%$ .

The ground-state decay properties of  $^{266}106$  should be a quite sensitive probe of the theoretical predictions shown in Fig. 1. If there is increased stability near  $N=162$  and  $Z=108$ , the isotope  $^{266}106$  should have a SF- or  $\alpha$ -decay half-life of tens of seconds. Otherwise,  $^{266}106$  should decay by SF with a half-life of  $\sim 100$   $\mu$ s, a  $T_{sf}$  difference of  $\sim 10^5$ . Thus a distinct signature for enhanced nuclear stability near  $N=162$  and  $Z=108$  would be the observation of the  $\alpha$  decay of  $^{266}106$  followed by the SF decay of the daughter nucleus  $^{262}104$ . A signature for the odd- $A$  isotope  $^{265}106$  would be the observation of its  $\alpha$  decay followed by  $\alpha$  decays of the known nuclides  $^{261}104$  and  $^{257}102$ .

To produce  $^{265}106$  and  $^{266}106$  we used the complete fusion reaction  $^{248}\text{Cm} + ^{22}\text{Ne}$  at bombarding energies of 116 and 121 MeV which are expected to provide maximum cross sections for the 4n and 5n evaporation channels. Beams of  $^{22}\text{Ne}$  projectiles from the U400 cyclotron of the Joint Institute for Nuclear Research passed through rotating 3- $\mu\text{m}$  Ti foils and curium targets (97%  $^{248}\text{Cm}$  and 3%  $^{246}\text{Cm}$ ). Three targets with average areal densities of 240  $\mu\text{g cm}^{-2}$  of  $^{248}\text{Cm}$  and a total area of 11.7  $\text{cm}^2$  were arranged on a wheel whose rotation was synchronized to the 150-Hz frequency of the cyclotron so that a target was exposed to the  $\sim 2$ -ms beam macropulse during each 6.7-ms beam cycle. The targets were electrodeposited on 710- $\mu\text{g cm}^{-2}$  Ti foils and covered by a 30- $\mu\text{g cm}^{-2}$  carbon layer. We obtained a total beam dose of about  $1.6 \times 10^{19}$  particles with typical intensities of  $1.3 \times 10^{13}$  pps of  $^{22}\text{Ne}$ .

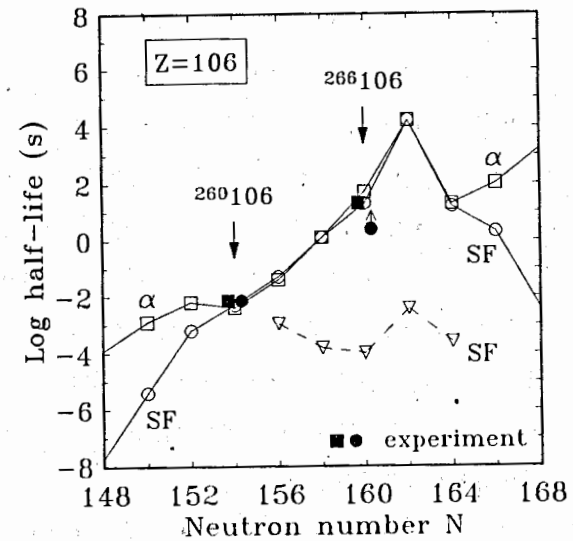


FIG. 1. Predicted partial half-lives [4] for SF and  $\alpha$  decay of the even-even 106 isotopes shown by the lines connecting circles and squares, respectively. The dashed line connecting the triangular points shows SF half-life predictions [5]. The experimental values for  $^{260}106$  [7,10] and the results for  $^{266}106$  from this work are shown for comparison.

Evaporation residues (EVRs) recoiling out of the  $^{248}\text{Cm}$  targets were separated in-flight from beam particles and transfer products by the Dubna gas-filled recoil separator described in Ref. [11]. The separator was filled with hydrogen at a pressure of 0.7 Torr. We set the magnetic rigidity of the separator's dipole magnet for the slow  $Z=106$  EVRs according to prior measurements [11] of the average charge state in hydrogen,  $\langle q \rangle$ , for the slow EVRs with  $Z=100, 102, \text{ and } 104$  produced in the reactions  $^{235}\text{U} + ^{18}\text{O}$ ,  $^{235}\text{U} + ^{22}\text{Ne}$ , and  $^{242}\text{Pu} + ^{22}\text{Ne}$ . The separated EVRs passed through a time-of-flight (TOF) measurement system composed of two multiwire proportional chambers in a 1-Torr pentane-filled module and were finally implanted in a position-sensitive surface-barrier detector (PSD) array.

The PSD array consisted of three surface-barrier detectors, with each detector having eight 40-mm high  $\times$  4.8-mm wide strips. We obtained horizontal positions for the reaction products from the 24 strips and vertical positions from the 40-mm high resistive back of the detectors. A particle striking a detector generated a signal in a strip and in the resistive back of the detector. Signals from the detector strips were processed for  $\alpha$  and implant energies. Top and bottom signals from the back of each detector were split into two channels to provide position signals in the 40-mm direction for  $\alpha$ /implant events ( $\sim$ 0.5 to 15 MeV) and fission events (15 to 200 MeV). We calculated total fission energies by summing the position energy signals. With each detected event, we also recorded the strip number, TOF information, beam current, the time in  $\mu$ s from beginning of each beam pulse to either  $\alpha$ /implant or fission events, and the time since the beginning of the data acquisition cycle in 0.1-ms intervals. The data were accumulated in list mode in an LSI 11/73 computer and periodically transferred to a microVAX computer for storage and off-line analysis.

Alpha-energy calibrations were performed for each strip using the  $\alpha$  peaks from nuclides produced in the  $^{197}\text{Au} + ^{22}\text{Ne}$  reaction. Most of the strips had energy resolutions of about 100 keV. An approximate fission-energy calibration was obtained by extrapolating the  $\alpha$ -energy calibration and by setting the separator magnetic rigidity so that  $^{22}\text{Ne}$  projectiles of known energy impinged upon the detectors. We also performed a calibration bombardment of  $^{235}\text{U}$  with  $1.3 \times 10^{18}$  particles of  $^{22}\text{Ne}$  to measure the  $\alpha$  and SF activities from the known nuclide  $^{252}\text{102}$  and to estimate the EVR collection efficiency. We used known  $\alpha$ - $\alpha$ , EVR- $\alpha$ , and EVR-SF sequences from the calibration reactions to estimate FWHM position resolutions of  $\sim$ 3% of the strip length for the  $\alpha$ - $\alpha$  sequences and  $\sim$ 9% for  $\alpha$ -SF or EVR- $\alpha$  sequences.

We had low efficiencies for detecting EVRs because the initial  $Z=106$  EVR energy of 7 MeV was reduced to  $\sim$ 2 MeV implantation energy due to losses in the target, hydrogen gas, and the TOF module. The measured energy was expected to be about half the implantation energy due to the pulse-height defect and losses in the detector dead layer. This resulted in most of the EVR signals being below the detection threshold.

In the off-line analyses we searched for time and position correlated  $\alpha$ -SF and  $\alpha$ - $\alpha$  event chains. We list in Table I the observed  $\alpha$ -SF and  $\alpha$ - $\alpha$  correlations. The out-of-beam counting rate for  $\alpha$ 's in the energy range of interest (Fig. 2) and for SF events (Fig. 3) was extremely low,  $\sim$ 1 event per day per strip regardless of the bombarding energy, providing a very high statistical significance for all the correlations in Table I. Using our data we calculated the probabilities that the 4 out-of-beam  $\alpha$ -SF correlations and the 2  $\alpha$ -SF correlations with the  $\alpha$  in-beam, are of random origin are less than  $10^{-15}$  and less than  $10^{-4}$ , respectively.

We attribute the six  $\alpha$ -SF event pairs at 116 and 121 MeV with a maximum likelihood result of  $E_{\alpha} = 8.63 \pm 0.05$  MeV to the decay chain  $^{266}\text{106} \Rightarrow ^{262}\text{104}$  for which we measured a production cross section of 80 pb at 116 MeV and 60 pb at 121 MeV. We assigned the four  $\alpha$ - $\alpha$  correlations at 121 MeV with  $E_{\alpha 1} = 8.71$  to 8.91 MeV to the decay chain  $^{265}\text{106} \Rightarrow ^{261}\text{104}$  ( $T_{1/2} = 65$  s,  $E_{\alpha} \sim 8.29$  MeV)  $\Rightarrow ^{257}\text{102}$  ( $T_{1/2} = 26$  s,  $E_{\alpha} \sim 8.22, 8.27, 8.32$  MeV) for which we measured a production cross-section of 260 pb. The cross sections are reported with an estimated accuracy of a factor of  $\sim$ 3. We attribute the 8.16- to 8.17-MeV  $\alpha$ - $\alpha$  correlation to the decay chain  $^{261}\text{104} \Rightarrow ^{257}\text{102}$ . We note that except for the triple correlation, one cannot distinguish between  $^{261}\text{104}$  and  $^{257}\text{102}$  due to their similar  $\alpha$  energies and half-lives.

TABLE I. The measured parameters of the  $\alpha$ -SF and  $\alpha$ - $\alpha$  correlation chains observed in the  $^{248}\text{Cm} + ^{22}\text{Ne}$  reaction. All events are out-of-beam except for those three indicated.

Decay mode	Particle energy, MeV*	Strip number	Time interval	Position deviation, mm
<b>116 MeV</b>				
$\alpha$	8.60	16		
SF	105	16	191 ms	3.0
$\alpha$	8.54	22		
SF	89	22	215 ms	3.0
$\alpha$	8.59	24		
SF	96	24	748 ms	1.3
$\alpha$	8.74	21		
SF	118	21	6453 ms	1.8
<b>121 MeV</b>				
$\alpha^\dagger$	8.69	11		
SF $^\dagger$	103	11	360 ms	0.3
$\alpha^\dagger$	8.60	13		
SF	118	13	2011 ms	1.8
$\alpha$	8.85	21		
$\alpha$	8.20	21	3 s	0.8
$\alpha$	8.81	1		
$\alpha$	8.31	1	334 s	0.3
$\alpha$	8.17	1	60 s	1.0
$\alpha^\ddagger$	8.91	1		
$\alpha$	8.12	1	86 s	?
$\alpha$	8.71	12		
$\alpha$	8.14	12	20 s	0.2
$\alpha$	8.16	8		
$\alpha$	8.17	8	1 s	0.7

\* The quoted fission fragment energies are measured values. No estimate was included for the pulse-height defect or the fraction of the total kinetic energy deposited in the detectors.

$^\dagger$  Event occurred during the beam pulse.

$^\ddagger$  Position signals were not detected for this event.

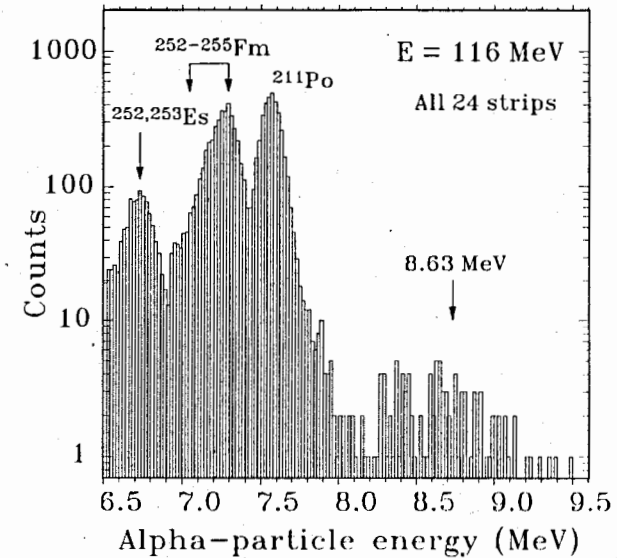


FIG. 2. Out-of-beam  $\alpha$ -energy spectrum from all detectors at 116 MeV ( $1.0 \times 10^{19}$  particles  $^{22}\text{Ne}$ ). The spectrum at 121 MeV ( $0.6 \times 10^{19}$  particles  $^{22}\text{Ne}$ ) is very similar.

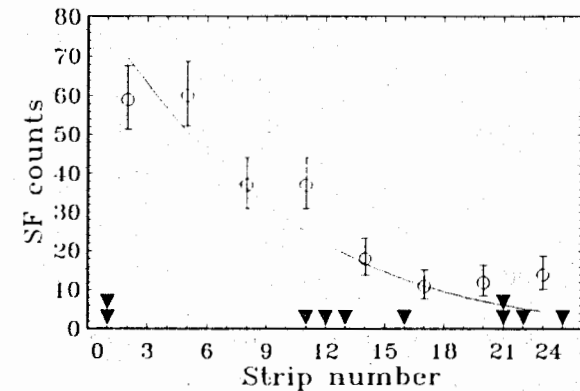


FIG. 3. The distribution of all detected 248 out-of-beam SF events at 116 MeV. Events from each three adjacent strips are summed. The distribution at 121 MeV is very similar. The curve is a Gaussian fit to the distribution across the strips of the Fm  $\alpha$ -events shown in Fig. 2. The triangles show the location of the  $\alpha$ -SF and  $\alpha$ - $\alpha$  ( $\alpha$ ) correlations from both the 116 and 121 MeV bombardments.

Our assignment of the six  $\alpha$ -SF correlations to the decay of  $^{266}106$  is based on the following observations. The  $\alpha$ -SF correlation chains with  $E_\alpha = 8.63$  MeV and short time intervals from 0.2 to 6.5 s are unique; for the synthesis reaction that we employed, one cannot identify any candidate  $\alpha$ -SF decay sequences with other  $Z, A$  values which would have similar decay properties. Furthermore, the 8.63-MeV  $\alpha$  energy is in agreement with both predictions and systematics as is the SF decay mode for the  $Z=104$  daughter. The six  $\alpha$ -SF correlation chains were detected by using the gas-filled recoil separator which strongly suppresses beam particles and many kinds of background reaction products relative to compound nucleus products. The  $\alpha$ -SF and  $\alpha$ - $\alpha$  chains were broadly distributed across the detector array as expected for products of the ( $^{22}\text{Ne}, 4\text{-5n}$ ) reactions, while the largest number of single SF and  $\alpha$  events, which come from transfer products like  $^{256}\text{Fm}$  and lighter Fm isotopes, occurred closer to the end of the detector array that corresponds to lower magnetic rigidity values (Fig. 3). From our data, we estimated the average charge state  $\langle q \rangle$  of the slow  $Z=106$  EVRs in hydrogen to be  $2.0^{+0.2}_{-0.3}$  at  $\langle v/v_0 \rangle \approx 1.0$  ( $v_0 = 2.2 \times 10^6$  m s $^{-1}$  is the Bohr velocity), in full agreement with the previous  $\langle q \rangle$  measurements [11] for  $Z=100$  through 104. Finally, the production cross sections for the  $\alpha$ -SF correlations at both 116 and 121 MeV agree with systematics.

We assigned the four  $\alpha$ - $\alpha$  correlations with  $E_{\alpha 1} = 8.71$  to 8.91 MeV to the decay of  $^{265}106$  using arguments similar to those given above for  $^{266}106$ . Especially convincing is the triple- $\alpha$  correlation.

The above observations and arguments provide consistent evidence for the assignment of the correlation chains to the  $\alpha$  decay of  $^{265}106$  and  $^{266}106$ . The correlation times for the six  $\alpha$ -SF chains give a half-life of  $1.2^{+1.0}_{-0.5}$  s (Fig. 4) for  $^{262}104$ . A SF activity with  $T_{1/2} \sim 47$  ms was tentatively assigned by Somer-

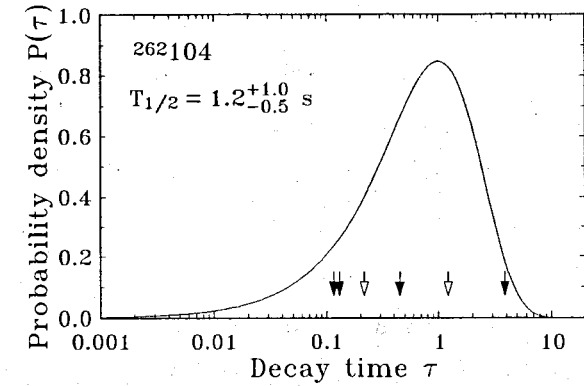


FIG. 4. The probability density  $P(\tau) = (\tau/n10)e^{-\tau}$  vs. the decay time  $\tau = (t \ln 2)/T_{1/2}$  for the six correlations. Solid and open arrows show the  $\tau$  values for the  $\alpha$ -SF correlations from the 116 and 121 MeV bombardments, respectively.

ville *et al.* [12] to  $^{262}104$ . In fact, an unassigned 1.3-s SF activity was also produced at the near-barrier bombarding energies 89 and 95 MeV in the  $^{248}\text{Cm} + ^{18}\text{O}$  reaction [12]. Moreover, Hoffman *et al.* [13] produced a 1.5-s SF activity and measured its fission properties in the same  $^{248}\text{Cm} + ^{18}\text{O}$  reaction at 95 MeV. Our findings establish that the total half-life of the ground state decay of  $^{262}104$  is 1.2 s. An explanation of the 47 ms SF activity could be associated with the presence of a quasiparticle K-isomeric state in  $^{262}104$  (or in a nearby nuclide), as discussed in Refs. [14,15].

We estimated the partial  $\alpha$ -decay half-lives of  $^{265,266}106$  from the measured  $\alpha$ -decay energies. Since  $^{266}106$  is even-even, its  $\alpha$  decay will be ground-state to ground-state and the estimation is straightforward. Using the phenomenological formula of Viola and Seaborg in Ref. [3], we determined a partial  $\alpha$  half-life for  $^{266}106$  of 10 to 30 s. Similarly, we obtained an  $\alpha$  half-life of 2 to 30 s for  $^{265}106$  assuming a hindrance factor between 1 and 3.

The  $\alpha$ -branching ratios are probably  $\geq 50\%$  for both 106 nuclides based on our cross-section evaluations which are about the expected values for the 4n and 5n evaporation channels. We set a very conservative  $\alpha$ -branching lower limit of 15% for  $^{266}106$  from the beam-off data at 116 MeV by assuming that all of the observed fissions detected in strips numbered 16 to 24 (Fig. 3) are from the SF decay of  $^{266}106$  or its daughter,  $^{262}104$ . Most of the observed SF events are actually from the transfer product  $^{256}\text{Fm}$ , based on their distribution across the strips and on their yield compared to that of  $\alpha$ -emitting Fm isotopes [16].

The ground-state decay properties that we established for  $^{266}106$  reveal a significantly increased stability near  $N=162$  and  $Z=108$  and are in agreement with the theoretical predictions made in Refs. [1-4]. The half-life of 1.2 s for  $^{262}104$  also signals the trend toward greater nuclear stability with  $N$  approaching 162. The short SF half-lives predicted by Möller *et al.* [5] are inconsistent with our results.

The discovery of the significant nuclear stability near  $N=162$  and  $Z=108$  reported in the present paper creates new opportunities for many further explorations at the edge of the nuclear domain.

We wish to thank the U400 cyclotron staff for providing these long-term bombardments with the intense  $^{22}\text{Ne}$  beams. We take pleasure in thanking V.V. Bekhterev and I.V. Kolesov for their essential contributions to the development of the gas-filled separator, V.I. Krashonkin for his skillful technical assistance, and L.I. Salamatin for his help in electroplating the curium targets. Our debt concerning this work is owed to the late V.M. Plotko, whose ingenious care of the experimental technique was invaluable. We thank E.D. Watkins and D.H. Tinoco for development of the electronics system and J.T. Walton for producing the position sensitive detectors. Three of us (RWL, KJM, and JFW) thank the Joint Institute for Nuclear Research for its hospitality during the course of the experiments. The curium target material supplied by the Liver-

more collaborators was provided by the Office of Basic Energy Sciences, U.S. Department of Energy, through the transplutonium production facilities of the Oak Ridge National Laboratory. Most of the support of the Livermore collaborators was provided through the U.S. Department of Energy by the Lawrence Livermore National Laboratory under contract No. W-7405-Eng-48. These studies were performed in the framework of the US/Russian Federation Joint Coordinating Committee for Research on Fundamental Properties of Matter.

#### REFERENCES

- [1] S. Čwiok, V.V. Pashkevich, J. Dudek, and W. Nazarewicz, *Nucl. Phys.* A410, 254 (1983).
- [2] Z. Patyk, J. Skalski, A. Sobiczewski, and S. Čwiok, *Nucl. Phys.* A502, 591c (1989).
- [3] Z. Patyk and A. Sobiczewski, *Nucl. Phys.* A533, 132 (1991).
- [4] A. Sobiczewski, presented at Actinides-93 Conf., September 19-24, 1993, Santa Fe, NM.
- [5] P. Möller, J.R. Nix, and W.J. Swiatecki, *Nucl. Phys.* A469, 1 (1987); *Nucl. Phys.* A492, 349 (1989); P. Möller and J.R. Nix, *Nucl. Phys.* A549, 84 (1992).
- [6] R.W. Lougheed, E.K. Hulet, J.F. Wild, K.J. Moody, R.J. Dougan, C.M. Gannett, R.A. Henderson, D.C. Hoffman, and D.M. Lee, *Fifty Years with Nuclear Fission*, Vol. 2, American Nuclear Society, La Grange Park, IL, 1989, p. 694.
- [7] G. Münzenberg, S. Hofmann, H. Folger, F.P. Hessberger, J. Keller, K. Poppensieker, B. Quint, W. Reisdorf, K.-H. Schmidt, H.J. Schött, P. Armbruster, M.E. Leino, and R. Hingmann, *Z. Phys.* A322, 227 (1985).
- [8] A. Ghiorso, J.M. Nitschke, J.R. Alonso, C.T. Alonso, M. Nurmi, G.T. Seaborg, E. K. Hulet, and R.W. Lougheed, *Phys. Rev. Lett.* 33, 1490 (1974).
- [9] Yu.Ts. Oganessian, Yu.P. Tretyakov, A.S. Iljinov, A.G. Demin, A.A. Pleve, S.P. Tretyakova, V.M. Plotko, M.P. Ivanov, N.A. Danilov, Yu.S. Korotkin, and G.N. Flerov, *Zh. Eksperim. Theor. Fiz. Pis'ma* 20, 580 (1974) [*Sov. JETP Letters* 20, 265 (1974)].
- [10] A.G. Demin, S.P. Tretyakova, V.K. Utyonkov, and I.V. Shirokovsky, *Z. Phys.* A315, 197 (1984).



- [11] Yu.A. Lazarev, Yu.V. Lobanov, A.N. Mezentsev, Yu.Ts. Oganessian, V.G. Subbotin, V.K. Utyonkov, F.Sh. Abdullin, V.V. Bekhterev, S. Iliev, I.V. Kolesov, A.N. Polyakov, I.M. Sedykh, I.V. Shirokovsky, A.M. Sukhov, Yu.S. Tsyganov, and V.E. Zhuchko, in *Heavy Ion Physics, Scientific Report 1991-1992*, JINR Report No. E7-93-57, Dubna, 1993, p. 203; in *Proc. Int. School-Seminar on Heavy Ion Physics, Dubna, 1993*, JINR Report No. E7-93-274, Dubna, 1993, Vol. 2, p. 497.
- [12] L.P. Somerville, M.J. Nurmia, J.M. Nitschke, A. Ghiorso, E.K. Hulet, and R.W. Lougheed, *Phys. Rev. C* **31**, 1801 (1985); L.P. Somerville, Ph.D. thesis, University of California, Report No. LBL-14050, Berkeley, 1982.
- [13] D.C. Hoffman, D. Lee, A. Ghiorso, M.J. Nurmia, K. Aleklett, and M. Leino, *Phys. Rev. C* **24**, 495 (1981).
- [14] Yu.A. Lazarev, *Phys. Scripta* **35**, 255 (1987).
- [15] Yu.A. Lazarev, Yu.V. Lobanov, R.N. Sagaidak, V.K. Utyonkov, M. Hussonnois, Yu.P. Kharitonov, I.V. Shirokovsky, S.P. Tretyakova, and Yu.Ts. Oganessian, *Phys. Scripta* **39**, 422 (1989).
- [16] D. Lee, H. von Gunten, B. Jacak, M. Nurmia, Y. Liu, C. Luo, G.T. Seaborg, and D.C. Hoffman, *Phys. Rev. C* **25**, 286 (1982).

Received by Publishing Department  
on March 11, 1994